Measurement and calculation of guide vane performance in expanding bends for wind-tunnels

B. Lindgren, J. Österlund, A. V. Johansson

Abstract The design of guide vanes for use in expanding bends was investigated both experimentally and numerically. The primary application in mind is the use of expanding corners in wind-tunnels for the purpose of constructing compact circuits with low losses. To investigate the performance of guide vanes in realistic situations expansion ratios between 1 and $\frac{5}{3}$ were tested in the experiments. These were carried out in an open wind-tunnel specially built for the present purpose. The experimental results demonstrated that suitably designed guide vanes give very low losses and retained flow quality even for quite substantial expansion ratios. For wind-tunnel applications expansion ratios around 1.3 seem appropriate, Optimization of a guide vane design was done using a two-dimensional cascade code, Mises. A new vane optimized for an expansion ratio of $\frac{4}{3}$ gave a two-dimensional total pressure-loss coefficient as low as 0.041 for a chord Reynolds number of 200,000.

1
Introduction
In closed wind-tunnels the requirement of attached flow in the diffusers is often a major factor in determining the total length of the circuit. In the present work we investigate the idea of using expanding corners equipped with guide vanes to reduce the need for diffusers in wind-tunnel applications. Actually, the use of expanding corners could also be of interest in various other applications, such as ventilation systems.

Expanding corners with low losses would both reduce the total losses and give the possibility of increasing the length of the test section for a given circuit length. Space restrictions are often serious limiting factors when wind-tunnels are designed. Expanding corners offer a promising way to obtain a compact circuit if a good performance of the guide vanes can be guaranteed.

Many wind-tunnels use $\frac{1}{4}$-circle-shaped vanes with prolongation at the trailing edge. Such vanes have a three-dimensional total pressure-loss coefficient of typically 0.20, see Klein et al. (1930). This is about 4 times as much as for an optimized profile. It is not, however, always the lowest pressure-loss coefficient that is desirable. Also good flow quality is essential, especially in the corner upstream of the setting chamber.

The present work includes both an experimental and a numerical investigation of guide vane performance in expanding 90° bends. The experiments cover a range of Reynolds numbers, vane spacings and area ratios. The numerical calculations were done both for comparison with the experimental results and to optimize a new vane for expanding corners.

The experiments were performed in a small test tunnel built specifically for this purpose. It is an open tunnel, with a 300×300 mm² straight section upstream of the corner connected to the downstream variable area section. The tests covered a chord Reynolds number range up to 230 000. The total pressure-loss coefficient was determined and the behaviour of the flow was studied with the aid of smoke visualization.

During the construction of the MTL wind-tunnel at KTH a guide vane was developed and optimized for a non diffusing corner at low Reynolds numbers. A first part of this study is reported by Sahlin and Johansson (1991), pertaining to vanes designed to have turbulent boundary layers. The ones finally used in the MTL-tunnel at KTH were designed to have laminar boundary layers. An already good understanding of its behaviour and the very low pressure-loss achieved in a corner using this vane made it suitable for the new application. The two-dimensional pressure loss coefficient is below 0.04 for this vane at a chord Reynolds number of 200,000.

These vanes were tested in expanding corners and found to give quite satisfactory results. A new vane was also designed and optimized for the situation in an expanding corner.

The present results will be used in the construction of a new wind-tunnel at KTH, where the corner expansions are used to accommodate a total area expansion of a factor of three. Plane diffusers, with the expansion only in the direction normal to the plane of the tunnel circuit, are then used to give a further area increase by a factor of three. Hence, a total contraction ratio of nine is achieved with a quite moderate need of diffusers, yet with an expansion ratio of about 1.32 in each

B. Lindgren, J. Österlund, A. V. Johansson
Royal Institute of Technology
Department of Mechanics
SE-100 44 Stockholm, Sweden

Correspondence to: A. V. Johansson

corner. The results presented in this work show that this can be achieved with very small losses in the corners, and a good quality of the flow exiting the corners.

2
Methods of calculating total pressure-loss coefficient and lift coefficient

When the flow passes through a sharp bend equipped with guide vanes, the pressure field is set up by the ensemble of vanes and the walls. Hence, instead of analyzing a single vane, one has to analyze a cascade of vanes.

2.1
The total pressure-loss coefficient

The quantities needed to be measured in the experiments are the difference between total and static pressure at position 1 and the difference between atmospheric pressure and static pressure at position 0 and 1, respectively. Position 0 is located upstream of the corner and position 1 is located downstream of the corner (see Fig. 1).

The total pressure-loss coefficient is defined as

$$\frac{\Delta H}{q_0} = \frac{p_{t0} - \overline{p_{t1}}}{q_0} \tag{1}$$

where p_{t0} is the total pressure at position 0 and $\overline{p_{t1}}$ is the mean value of the total pressure over the cross-section at position 1. ΔH is the average total pressure-loss in the corner and q_0 is the dynamic pressure at position 0. The dynamic pressure at position 0 is defined as

$$q_0 = \tfrac{1}{2} \rho U_0^2 \tag{2}$$

where U_0 is the flow velocity at position 0. The mean value of the total pressure at position 1 is

$$\overline{p_{t1}} = \frac{1}{nh_1} \int_0^{nh_1} p_{t1}(y) \, dy \tag{3}$$

where n is the number of vanes over which the integration is performed and h_1 is the spacing between the vanes perpendicular to the outflow direction, see Fig. 2.

If the frictional resistance in the inlet is neglected Bernoulli's theorem gives that q_0 is the difference between the atmospheric pressure and the static pressure at position 0. Hence,

$$q_0 = p_{atm} - p_0 \tag{4}$$
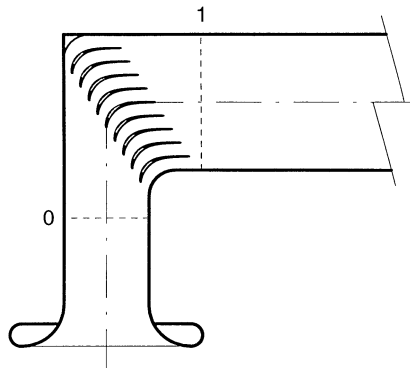
Fig. 1. The guide-vane corner with the measurement positions 0 and 1
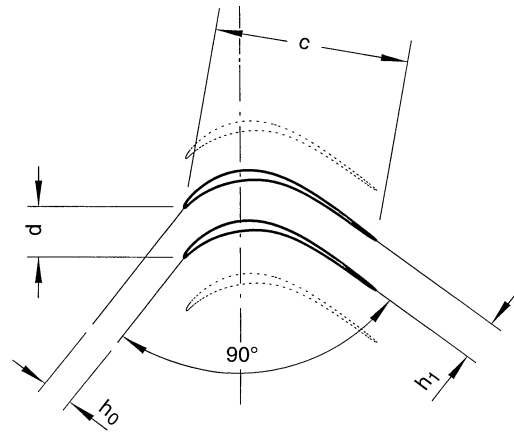
Fig. 2. The cascade geometry

The same reasoning yields that the total pressure at position 0, p_{t0}, is equal to the atmospheric pressure,

$$p_{t0} = p_{atm} \tag{5}$$

Combining Eqs. (1), (3), (4) and (5) results in the following expression for the total pressure-loss coefficient written on a form displaying the pressure differences measured in the experiments,

$$\frac{\Delta H}{q_0} = \frac{p_{atm} - p_1 - \frac{1}{nh_1} \int_0^{nh_1} (p_{t1}(y) - p_1) y}{p_{atm} - p_0} \tag{6}$$

2.2
Calculation of lift coefficient

From the momentum theorem, the following expression for the lift-force on a 90° expanding bend, can be derived.

$$L' = 2q_0 \frac{d}{e} \tag{7}$$

where L' is the lift force per unit length in the spanwise direction and d is the spacing between the vanes, see Fig. 2. The expansion ratio, e, is defined as

$$e = \frac{h_1}{h_0} \tag{8}$$

where h_0 and h_1 is the spacing between the vanes perpendicular to the inflow and outflow directions respectively, see Fig. 2.

The total pressure-loss over the cascade, ΔH, is

$$\Delta H = \frac{D'}{d} \tag{9}$$

where D' is the drag per unit length in the spanwise direction.

This results in the following expression for the total pressure-loss coefficient,

$$\frac{\Delta H}{q_0} = \frac{2}{e} \frac{D'}{L'} \tag{10}$$

Note that the lift-to-drag ratio in equation (10) refers to the entire corner and not just a single vane. In other words it

is important not only to maximize the lift-to-drag ratio for a single vane but also to reduce the number of vanes needed in the cascade.

The dimensionless lift coefficient is defined as

$$c_{L'} = \frac{L'}{1/2\,\rho c u^2} \qquad (11)$$

where c is the vane chord and u is the flow speed over the vanes. The question is now which flow speed is the most representative for this case. The most important factor affecting the flow characteristics is obviously separation, which normally will start at the trailing edge of the vane (Fig. 2). Therefore the flow speed at the trailing edge is chosen for normalization in expression (11). It now reads

$$c_{L'} = \frac{L'}{1/2\,\rho c (U_o/e)^2}. \qquad (12)$$

Introducing the dimensionless pitch, ε, defined as the vane spacing to chord ratio,

$$\varepsilon = \frac{d}{c} \qquad (13)$$

results, together with Eqs. (2), (7) and (12), in the following equation for the lift coefficient

$$c_{L'} = 2\varepsilon e. \qquad (14)$$

3
Experimental apparatus
The wind tunnel, see Fig. 3, used in the experiments was constructed especially for this purpose, although the fan with upstream and downstream silencers existed as parts of an older test rig.

3.1
The wind-tunnel used in the experiments
The tunnel is of the open-suction-type with an inlet equipped with a contraction (1), (numbers referring to Fig. 3), with an area ratio of 9.

The straight section upstream of the corner, (2), has an area of 300×300 mm² and a length of about 400 mm to ensure uniform inflow conditions for the corner vanes. In this section the static wall pressure is measured at a location 300 mm downstream of the inlet, at half tunnel height. Extra care has been taken to achieve good quality pressure taps. This is very important when measuring static pressure (Shaw, 1960).

The 90° corner, (3) has a constant inlet area, and is adaptable to the expansion ratios, $1, \frac{4}{3}, \frac{3}{2}, \frac{5}{3}$ by varying the outlet width to 300, 400, 450 and 500 mm, respectively, keeping the tunnel

height constant at 300 mm. The corner walls are given a radius of curvature of 77.5 mm.

The guide vanes (91L198) tested are of the same design, although somewhat smaller than those used in the MTL low turbulence wind-tunnel at KTH. They are optimized for a non-expanding corner with a pressure-loss coefficient for such a situation that has been shown to be very small. They are made of aluminium extruded at SAPA, Sweden. Their span is 282 mm and the chord is 196 mm. This gives an aspect ratio of about 1.44 (Fig. 4).

To minimize the secondary flow over the vanes at this low aspect ratio, the wall boundary layers have to be controlled. This is achieved by separating the vanes 8 mm from the wall boundary layers. Small $\frac{1}{4}$-circle plates guide the boundary layer flow through the corner.

A mechanism enabled the angle of attack of the guide vanes to be easily adjustable in order to obtain the desired outflow angle which is achieved by measuring the static wall pressure 300 mm downstream from the corner.

The straight section downstream of the corner, (4), is made with an adaptive wall that enables the desired expansion ratio to be set. A pair of static wall pressure sensors is located 110 mm downstream from the inner radius at half tunnel height.

Sect. (5–9) include a diffuser, a transformation from a square to a circular cross section, silencers, a fan and another diffuser to increase the top speed of the wind-tunnel.

The speed range is from 0 to 25 m/s upstream of the corner giving a maximum chord Reynolds number of 325,000.

3.2
Measurement equipment
The measurements were made with a total pressure tube, 2 mm in diameter and 100 mm long. It was attached to a 400 mm long tube, 8 mm in diameter, which could be traversed in the cross-stream direction with a resolution of about 10 μm.
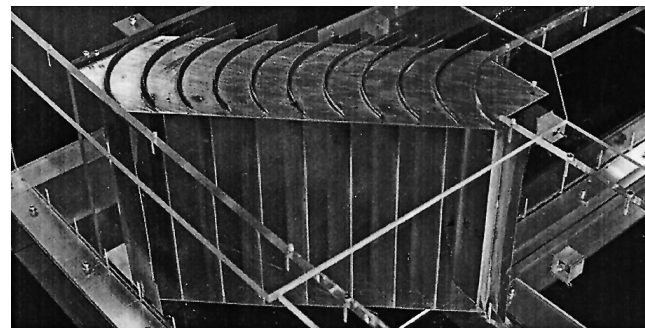
Fig. 4. The guide vanes at expansion ratio 1
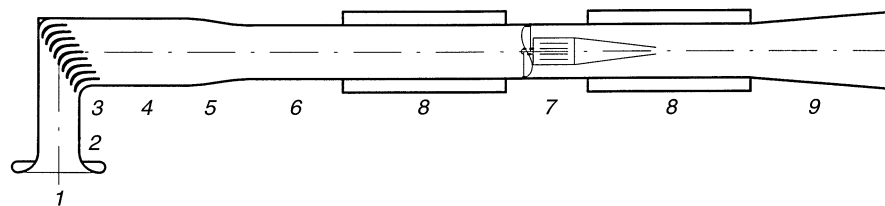
Fig. 3. The wind-tunnel used in the experiments. Expansion ratio $e = \frac{5}{3}$

A high accuracy (Furness Controll FC012) micro-manometer was used for the pressure measurements.

4
Measurements of the total pressure-loss coefficient

Four series of measurements were carried out to investigate the dependence of the two-dimensional total pressure-loss coefficient on the key flow parameters. First, measurements with a pitch (spacing to chord ratio) of 0.27 were made at the expansion ratios 1, $\frac{4}{3}$, $\frac{3}{2}$ and $\frac{5}{3}$. Then, two different expansions, $\frac{4}{3}$ and $\frac{3}{2}$, were used to investigate the effects of the Reynolds numbers in the range from 25,000 to 230,000. In a third series measurements the influence of the pitch was examined with the pitch ranging from 0.27 to 0.39. The aim was to find an optimum pitch for the expansion ratio $\frac{4}{3}$. The final type of comparative measurements studied the three expansion ratios, 1, $\frac{4}{3}$ and $\frac{3}{2}$, with the vanes having the same lift coefficient. The Reynolds number was 200,000 in all measurements except the Reynolds number variation experiment.

4.1
Variation of expansion ratio for constant pitch

The total pressure-loss coefficient increases with increasing expansion. There is reason to assume that the rate of increase becomes higher at large expansion ratios because of boundary layer separation on the vanes. In order to investigate this behaviour, expansion ratios as large as $\frac{5}{3}$ were tested.

A Reynolds number of 200,000 was selected because it is high enough to make the pressure loss fairly independent of small variations, but still low enough to represent typical flow speeds of low-speed wind-tunnels. In this case, with a vane chord of 196 mm, the velocity is about 15 m/s.

The pitch chosen is the same as in the MTL low turbulence wind-tunnel at KTH which is motivated by the fact that the vanes used in the experiments are of the same type as in that tunnel. The MTL-tunnel does not have expanding corners though. This pitch (0.27) is not an optimized value for the total pressure-loss coefficient, but is instead optimized for low disturbances in the flow and the vanes are thus able to take higher loads, occurring on expanding corners.

The results for different expansion ratios indicate indeed that there is a possibility to successfully incorporate the expanding corner element into the design of wind-tunnels (see Fig. 5). The results were very encouraging even at rather large expansion ratios. A more dramatic increase of the two-dimensional total pressure-loss coefficient was found only between the two highest expansion ratios.

The pressure distribution at position 1 is shown in Fig. 6 for an expansion ratio of $\frac{4}{3}$. For this expansion ratio flow over the vanes is essentially attached and the loss is only marginally higher than for the non-expanding case. The wake profiles for the largest expansion, on the other hand, indicate substantial separation of the vane boundary layers.

4.2
Variation of Reynolds number

The Reynolds number dependence of the total pressure-loss coefficient was studied at the two expansion ratios, $\frac{4}{3}$ and $\frac{3}{2}$. For non-diffusing corners with attached laminar flow on the vanes
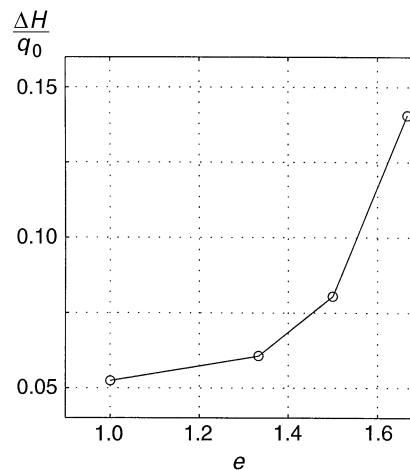
Fig. 5. The total pressure-loss coefficient as a function of the expansion ratio. $Re = 200,000$ and $\varepsilon = 0.27$
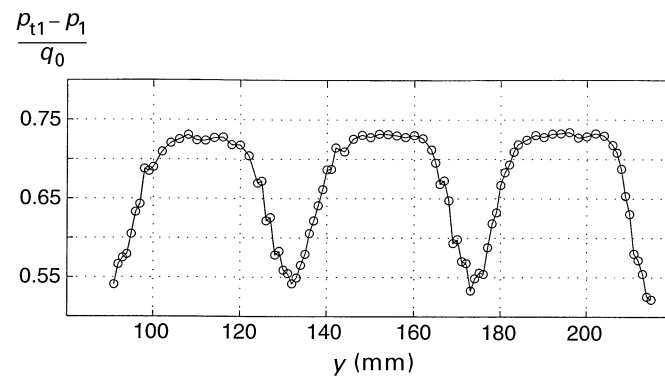
Fig. 6. Typical wake pressure distribution. $e = \frac{4}{3}$, $\varepsilon = 0.27$ and $Re = 200,000$

the normalized loss varies approximately as

$$\frac{\Delta H}{q_0} \sim \frac{1}{\sqrt{Re}} \tag{15}$$

The two measurement series with varying Reynolds numbers for expansion ratios of $\frac{4}{3}$ and $\frac{3}{2}$ gave similar results, although somewhat less favourable for the larger expansion, see Fig. 7. Hence, as might be expected, low-Reynolds number effects seem to be more severe at larger expansions.

At the lower Reynolds number studied, about 25,000, the flow speed is only 1 to 2 m/s which makes the measurements rather inaccurate and sensitive to disturbances caused by air movements in the laboratory outside the inlet of the open tunnel.

For the smaller expansion, $\frac{4}{3}$, we can observe a behaviour in Fig. 7 that is approximate in agreement with that expected from a completely laminar attached flow. Hence the slope is close to $-\frac{1}{2}$ in the log-log plot (cf Eq. (15)). At the higher expansion ratio the slope is smaller at low Reynolds numbers. Thereafter the total pressure-loss coefficient first begins to decrease faster than at lower Reynolds numbers, but with increasing Reynolds number the decrease in the value of the coefficient slows down again. An explanation for this behaviour could be that the flow is separated at low Reynolds
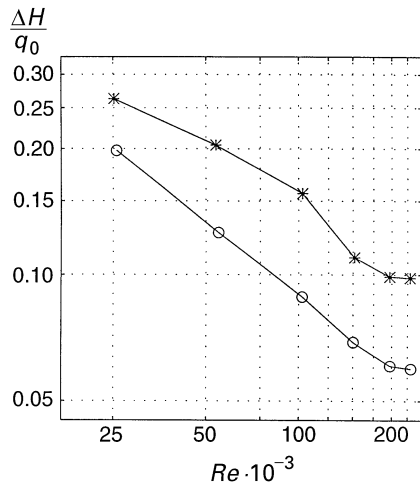
Fig. 7. The total pressure-loss coefficient as a function of the Reynolds number. $*$: $e = \frac{3}{2}$ and $\varepsilon = 0.24$, $\bigcirc$: $e = \frac{4}{3}$ and $\varepsilon = 0.27$

numbers, and at some higher value there is a reattachment creating a separation bubble. Downstream of the reattachment the flow is most probably turbulent, and the relative increase seen at high Reynolds numbers may then be interpreted as being caused by turbulent skin friction over an increasing part of the vane as the separation bubble becomes smaller. This behaviour would qualitatively explain the appearance of the curve for $\frac{3}{2}$ in Fig. 7, however this phenomenon has to be examined further.

4.3
Variation of pitch
The pressure-loss variation with pitch was investigated with the aim of finding an optimum at an expansion ratio in the range that would be of interest for wind-tunnel applications. This was chosen here as $\frac{4}{3}$. The optimum should be expected to vary somewhat with the expansion ratio. Actually a minimum of the total pressure-loss may not be the optimum solution in a more general sense since stability and flow quality also must be considered.

To find the vane spacing with the lowest value of the total pressure-loss coefficient, a series with the pitch ranging from 0.24 to 0.39 was performed. The results in Fig. 8 exhibit a minimum at a rather high value of the pitch, about 0.35. At this high value, the flow is most probably separated, but because of the thickness of the profiles and the frictional resistance they produce, a certain amount of separation leads to lower losses since fewer vanes are needed. The Reynolds number used here was 200,000. At lower Reynolds numbers separation tends to occur more easily, and the optimum value for the pitch will then be somewhat lower. The behaviour of the total pressure-loss coefficient as a function of the pitch indicates a sharp increase for pitch-values higher than the optimum value.

4.4
Variation of expansion ratio for constant lift coefficient
To best illustrate how the total pressure-loss coefficient varies with varying expansion ratio, one should perhaps make the comparison for equal loading of the vanes. By choosing $\varepsilon = 0.27$

for the expansion ratio $\frac{4}{3}$, we get a lift coefficient from Eq. (14) of 0.72, which should not be too high for this type of vane. With equal lift coefficient for the expansion ratios 1, $\frac{4}{3}$ and $\frac{3}{2}$ we obtain pitch values of 0.24, 0.27 and 0.36 for each expansion ratio, respectively.

Hence, in this measurement series the expansion ratio is varied under conditions such that the lift coefficient is held constant. This gives perhaps the most direct indication on how well every particular expansion functions. The increase in the total pressure-loss coefficient was found to be slightly stronger than in the case with the same pitch for every expansion, see Fig. 9. The Reynolds number was the same in both series, about 200,000, which enables a direct comparison between the results in Figs. 5 and 9.

4.5
Summary of the experimental results
It is clear from the above that the idea of expanding wind-tunnel corners works well if the expansion is not too large and the Reynolds number is kept reasonably high. A good
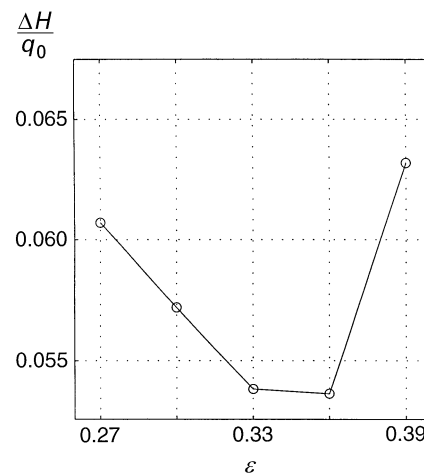
Fig. 8. The total pressure-loss coefficient as a function of the pitch. $e = \frac{4}{3}$ and $Re = 200{,}000$
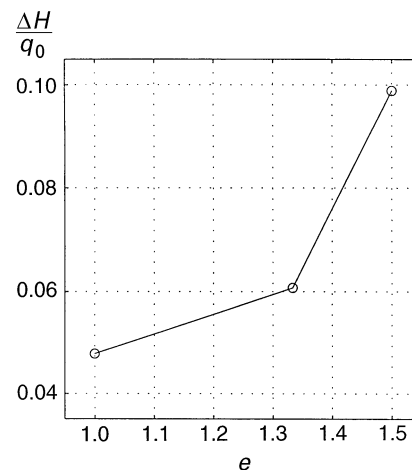
Fig. 9. The total pressure-loss coefficient as a function of the expansion ratio. $Re = 200{,}000$ and $c_{L'} = 0.72$

performance requires fairly well designed vanes but even vanes optimized for non-expanding corners can work well if designed to accommodate the lift coefficients occurring in the expanding corner.

With vanes optimized for a particular expansion the results will obviously be better. In the present investigation the vanes used were originally designed for non-expanding corners. A configuration with these vanes for an expansion ratio of $\frac{4}{3}$ and a pitch between 0.33 and 0.36 gives a total pressure-loss coefficient of less than 0.054 at a Reynolds numbers of about 200,000. A vane optimized for a non-diffusing corner was found by Sahlin and Johansson (1991) to give a two-dimensional total pressure-loss coefficient of about 0.036 at $Re = 154{,}000$. The increase in total pressure-loss is 50% for the expanding case.

If we choose to compare cases with equal lift coefficient, the $\frac{4}{3}$ expansion has a two-dimensional total pressure-loss coefficient of 0.061 to be compared with 0.048 for the non-expanding case, i.e. a 27% loss increase caused by the expansion.

We may also have in mind that typical vanes today in wind-tunnels are designed as $\frac{1}{4}$-circle-shaped vanes with prolongation at the trailing edge. For a non-expanding corner such vanes give a three-dimensional total pressure-loss coefficient of about 0.20, see (Klein et al. 1930).

5
Calculations of infinite cascade with experimental vane and vane optimization

Numerical calculations matching the Reynolds numbers and the expansion ratios with those in the experiments, give an opportunity to further study the values of the losses and pressure distributions around the vanes. They also provide information on the level of acuracy of the measurements.

Since the tested vane is optimized for non-expanding flows there are cases where parts of the flow are separated when the vane is used in an expanding corner. Abrupt increases of the pressure coefficient, C_p, in the pressure distribution of the vane will indicate where the separation takes place. A profile more optimized for an expansion ratio of $\frac{4}{3}$ is also developed.

5.1
The numerical code used in the calculations

The numerical calculations are made with the MISES code. MISES is a collection of programs for cascade analysis and design, including programs for grid generation and initialization, flow analysis, plotting and interpretation of results, and an interactive program to specify design conditions. MISES was developed by Harold Youngren and Mark Drela to analyze turbo-machinery design.

Mises first generates an incompressible 2-D panel solution to find the stagnation streamlines. It also locates iso-potentials at the vane edges. The streamlines and iso-potentials are used to generate the grid.

On the grid generated previously Mises solves steady Euler equations coupled with integral boundary layer equations using a Newton-Raphson method. This makes it possible to analyze flows with strong viscous/inviscid interactions like shock induced separation flows or separation bubbles. However, this requires the flow to be compressible. The minimum Mach number needed is in the range of 0.10–0.15. This is small

enough not to significantly affect the results for incompressible cases.

Optimizations of vane shapes can be performed with the help of an inverse method. Two different inverse methods are available, one suited for large modifications and one suited for detail modifications. In these methods the pressure distribution of the vane can be altered at wish and a number of modified Chebyshev polynomials are used to change the shape of the vane to fit the specified pressure distribution. These polynomials can be modified according to the users requests. The changes in the pressure distribution, however, has to be moderate to achieve convergence. This means that the optimization process has to be repeated a considerable number of times before major improvements are reached. It is also possible to edit the blade shape in the blade editor. However, only basic editing modes like rotate, translate and scale are available.

For further information on the Mises code see Youngren and Drela (1991), Drela and Youngren (1995), Giles and Drela (1987).

5.2
Calculations of infinite cascades with the experimental vane

The losses calculated in the MISES code are matching the losses obtained in the experiments quite well at moderate expansion ratios (see Fig. 10). However at higher expansion ratios the agreement is not very good. The losses from the computations show only a sight increase with increasing expansion ratio. Hence, the computations do not capture the large effects of separation at large expansion ratios. Three-dimensional effects will also disturb the two-dimensional measurements resulting in a faster increase of the losses than in the numerically calculated solutions which are purely two-dimensional.

The pressure distribution around the vane at the expansion ratio $\frac{4}{3}$ clearly indicates that it was not designed for expanding corners (see Fig. 11). On the lower surface there is a small separation bubble near the leading edge, and on the upper surface there is another but larger separation bubble about $\frac{1}{3}$
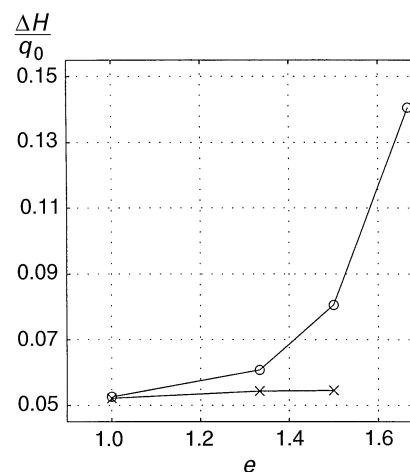
Fig. 10. The total pressure-loss coefficient as a function of the expansion ratio. $\varepsilon = 0.27$ and $Re = 200{,}000$. $\times$: computations, $\bigcirc$: experiments
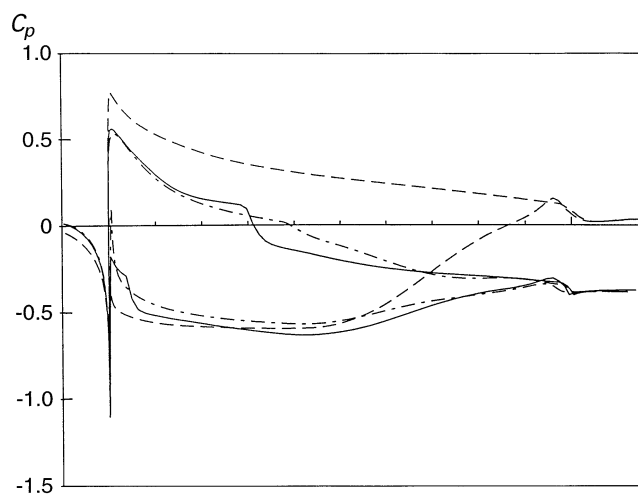
Fig. 11. Pressure distribution for 91L198 at $Re = 200{,}000$. Solid line: $e = \frac{4}{3}$ and $\varepsilon = 0.27$. Dashed line: $e = 1$ and $\varepsilon = 0.3$ (design point). Dash-dotted line: new vane (L27132B) with $e = \frac{4}{3}$ and $\varepsilon = 0.27$

Fig. 12. The total pressure-loss coefficient as a function of the angle of attack, α. $e = \frac{4}{3}$, $\varepsilon = 0.27$ and $Re = 200{,}000$

Fig. 13. Solid line: 91L198 optimized for non-expanding corners, $e = 1$ and $\varepsilon = 0.3$. Dashed line: L27132B the new vane optimized for expanding corners, $e = \frac{4}{3}$ and $\varepsilon = 0.27$

downstream of the leading edge. These features have a negative effect on the performance of the vane, and the losses can be reduced substantially in an optimization process.

The vane is also quite sensitive to variations in the angle of attack. Especially the first corner in a wind-tunnel is exposed to significant variations in the angle of attack where the disturbances from the test section are of considerable strength.

Numerical calculations with variations in the Reynolds number indicate an increase in the size of the separation bubbles with decreasing Reynolds number. The separation bubble on the upper surface also tends to move downstream with decreasing Reynolds number. For sufficiently small Reynolds number (or high loads), the flow will separate entirely from the vane. The MISES code is not able to reproduce this behaviour since it only accepts small wakes.

As long as the expansion ratio is moderate, the numerical calculations and the experimental results agree well. This means that the numerical calculation method can be used in the optimization process which could lead to a new profile design that better suits the particular conditions of expanding corners.

5.3
Optimization of a vane for the $\frac{4}{3}$ expansion ratio

When a new vane, emerging from the inverse process, fulfills the requirements of the designer one has to bear in mind that the profile is only optimized for the given Reynolds number, pitch, angle of attack and expansion ratio. To create a vane, that can be used under other circumstances than those specified in the optimization process, it is normally not meaningful to push the optimization too far for any given set of parameters. It is more important to assure that the vane can operate within a wide spectrum of flow conditions. This may lead to slightly larger losses but it will not have a major influence on, e.g., the overall losses of the wind tunnel.

The main goal of this optimization was to minimize and, if possible, eliminate all separation bubbles. The separation bubbles generate both transition from laminar to turbulent
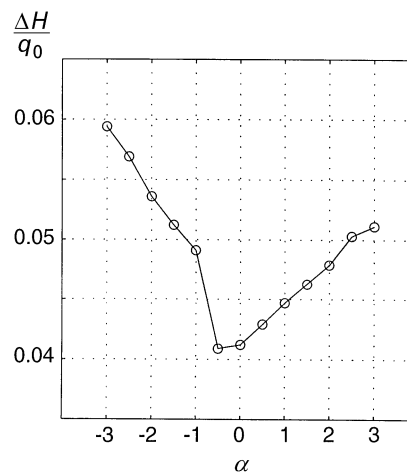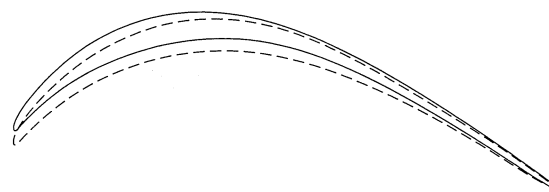
boundary layers and rapid increase in the pressure. With the new vane the influence of separation bubbles has been substantially reduced. (Fig. 11).

To improve the tolerance to variations in angle of attack the leading edge radius was enlarged. This resulted in a slightly larger total pressure-loss but increased the ability to perform with up to 3 degrees of negative angle of attack (Fig. 12).

The new vane is designed for a Reynolds number of 200,000, but it has been tested numerically for Reynolds numbers between 100,000 and 600,000. The total pressure-loss coefficient decreases rapidly with Reynolds number between 100,000 and 200,000, but for Reynolds numbers higher than 200,000 the decrease in total pressure-loss coefficient is small.

The conditions under which the optimization was performed is essential when comparing the results with other calculations or experiments. The Reynolds number, pitch and expansion ratio all have a strong impact on the final results, both in terms of losses and optimum vane shape. This new vane has a total presure-loss coefficient of 0.041 with a Reynolds number of 200,000, a pitch of 0.27 and an expansion ratio of $\frac{4}{3}$.

The differences in profiles of the experimentally tested vane and the new design, L27132B, suited for expanding corners are illustrated in Fig. 13. Coordinates representing the shape of the new vane can be found in Lindgren et al. (1997).

6
Discussion

Among early studies of guide vanes for corners in wind-tunnels we may mention (Collar, 1936; Klein et al. 1930; Kröber, 1932;

Wolf, 1957). An investigation of expanding corners that also include control of the boundary layers was carried out by Friedman and Westphal (1952). They studied a 90° cascade expanding bend with an area ratio of 1.45 : 1 and with several inlet boundary layers. Despite the rather simple design of the vanes used in that study quite promising results were obtained with a three-dimensional, but with thin boundary layers, total pressure-loss coefficient as low as 0.11. The total pressure-loss coefficient was almost independent of the Reynolds number that was varied between 330,000 and 950,000.

The present results show that a more sophisticated vane design can reduce this significantly and that it is indeed possible to construct expanding corners with small additional losses as compared to non-expanding ones.

This has several implications for the design of wind-tunnel circuits, but could also be used in a number of other applications, such as ventilation systems. For wind-tunnels it opens possibilities to substantially reduce the length of the return circuit without increasing the risk for separation in the diffusers. Actually, there are often conflicting requirements in connection with the construction of wind-tunnels to fit in the circuit within a given space and to have as large a test section as possible.

A possibility is also to reduce the total losses in the circuit by reducing wall friction losses and by enabling a larger cross sectional area at the second corner, thereby reducing the losses there. In traditional circuit design the diffuser between the first and second corner is quite short so that the second corner will have a cross sectional area not much larger than the first, and thereby comparable losses.

For large expansion ratios large regions of the flow will be separated, and the mean flow will be non-uniformly distributed with higher velocities near the inner radius. In the present study this phenomenon was visualized by smoke, which however was only possible at low Reynolds number (and may perhaps not be wholly representative for high Reynolds numbers). Also, three-dimensional secondary flow effects increase with increasing expansion. These drawbacks were quite negligible though at moderate expansion ratios, such as 1.33.

The geometry in an expanding corner is also somewhat different from an ordinary corner. In contrast to non-expanding corners the imaginary line from the centre of the inner radius to the centre outer radius does not go through the points where the straight walls meet. This means that the whole package of vanes is translated downstream in the tunnel. The relative position between the vanes also differs from the non-expanding case. This implies that there is room for significant improvements in the vane geometry from that optimized for the non-expanding situation. This was also clearly demonstrated by the new vane L27132B. Perhaps even better results can be achieved if the vane is designed to have

a turbulent boundary layer on the upper surface. With the fast increase in pressure along the chord which is a result of the expansion in the corner it is very difficult to maintain a laminar boundary layer on the upper surface. A vane designed to have turbulent boundary layers may therefore in some respects be a better starting-point in the optimization process.

The lift force on the vanes changes direction with changing expansion. This called for adjustments in the profile geometry. The absolute value of the lift force decreases with increasing expansion. This improves the efficiency of the expanding corner solution.

A suitable methodology that one may adopt in wind-tunnel circuit design with expanding corners is the following. Let us first define the x–y plane as the plane defined by the circuit centreline. For a given contraction ratio, C_R, and a contraction section with equal distortions in the two lateral directions, we can then choose to take the total x–y plane expansion, $\sqrt{C_R}$, in the corners, and the z-expansion in the diffusers. The diffusers will hence be plane with this approach, and will have a total area increase of a factor $\sqrt{C_R}$, only. The expansion in each corner becomes $C_R^{1/8}$ if the epansion is chosen to be the same in all corners. For instance, with a contraction ratio of 9, the expansion in each corner becomes approximately 1.32. This value will vary only slightly over the range of interesting contraction ratios because of the small value of the exponent $(\frac{1}{8})$.

Many alternative approaches are, of course, possible, depending on the design requirements in the specific case.

References

Collar AR (1936) Some experiments with cascades of aerofoils. A.R.C. Technical Report 1768. Aeronautical Research Committee

Drela M Youngren H (1995) A users guide to MISES 2.1. MIT Computational Aerospace Sciences Laboratory

Friedman D; Westphal WR (1952) Experimental investigation of a 90° cascade diffusing bend with an area ratio of 1.45 : 1 and with several inlet boundary layers. TN 2668, NACA

Giles MB; Drela M (1987) Two-dimensional transonic aerodynamic design method. AIAA J 25: 1199–1206

Klein GJ; Tupper KF; Green JJ (1930) The design of corners in fluid channels. Canadian J of Research 3: 272–285

Kröber G (1932) Schaufelgitter zur Umlenkung von Flüssigkeits-strömungen. Ingenieur-Archiv 3: 516–541

Lindgren B; Österlund J; Johansson AV (1997) Measurement and calculation of guide vane performance in expanding bends for wind tunnels. TRITA-MEK 1997:6, Department of Mechanics, KTH

Sahlin A; Johansson AV (1991) Design of guide vanes for minimizing the pressure loss in sharp bends. Phys Fluids A 3: 1934–1946

Shaw R (1960) The influence of hole dimensions on static pressure measurements. J Fluid Mech 7: 550–564

Wolf H (1957) Messungen im Nachlauf eines Gleichdruckgitters für 90°-Umlenkung. Maschinenbautechnik 6: 539–545

Youngren H; Drela M (1991) Viscous/inviscid method for preliminary design of transonic cascades. In: AIAA, SAE, ASME, and ASEE, Joint Propulsion, Conference, 27th